Dynamics of vertically vibrated two-dimensional granular layers

A. Alexeev, V. Royzen, V. Dudko, A. Goldshtein, and M. Shapiro*
Laboratory of Transport Processes in Porous Materials, Faculty of Mechanical Engineering, Technion–Israel Institute of Technology, Haifa, Israel

(Received 22 December 1997; revised manuscript received 20 July 1998)

Vibrational motion and dynamics of two-dimensional layers composed of identical inelastic solid disks are investigated experimentally and characterized in terms of the dimensionless acceleration. Several vibrational regimes with different degrees of vibrofluidization are studied by means of the layers' videorecordings and tracking the motion of one larger disk immersed into each bed of smaller particles. It is shown that depending on the vibrational acceleration, the larger disk either ultimately rises on top of the layer or vigorously moves throughout it, thereby indicating possibilities for efficient mixing. In a certain narrow range of the vibrational acceleration the layer is observed to repack and move as a single block. This acceleration range is well described by the model of an absolutely plastic body moving above a vibrated plate. Small deviations from this acceleration range lead to a significant layer expansion and distortion of its upper surface due to transverse waves. The vibrofluidization regimes are also characterized by measuring the force acting on the vessel's bottom and the time of its contact with the layer. The propagation speed of the compression-expansion waves is estimated and found consistent with the predictions of our earlier semiempirical and analytical models. [S1063-651X(99)11603-9]

PACS number(s): 81.05.Rm

I. INTRODUCTION

Moving granular materials are widely met in nature and technology [1]. The unusual cumulative properties of noncohesive flowing granules have attracted a lot of interest in recent years [2]. These materials flow like fluids, if external energy is continuously supplied, for example, by shearing or shaking. In other circumstances granular materials behave like solids.

This study is concerned with granular layers moving in a vertically vibrated container. Depending on the vibration parameters and the granular properties, such vibrated layers may move either as a single block or may show a variety of fluidlike phenomena such as surface waves [3–5], convection [6], transverse waves [7], and shock-expansion waves [8]. Vibrated granular layers were studied rather extensively in several works [3–8], aimed at investigating their basic physical behavior, as well as industrial applications [9–13], such as vibrotransport [12] and vibromixing [9].

In most vibrational regimes, achievable in commercially available vibrational stands, granular layers move as single solid bodies, which collide with the vessel as absolutely plastic blocks. This was observed even for layers composed of particles with very high restitution coefficient (up to 0.95) [10], because the granules rapidly lose kinetic energy of their random motion in the course of collisions. Only shallow layers [where the particles form not more that 6 monolayers (ML)] can be vibrofluidized to a significant measure, allowing implementation in technology [10]. However, even when the particles are vibrated seemingly as one solid block, their relative motion along closed loops can also be observed [6]. Yet the overall layer behavior can satisfactorily be described using the purely kinematic model of an absolutely plastic single block (see below).

The physical principles of vibrofluidization of thick granular layers have recently been described in [9]. It has been shown that by choosing appropriate vibrational regimes, one can increase the layer porosity even when the particles' restitution coefficient is low. Sometimes, such expanded layers still move in a way close to the predictions of the plastic body model (PBM). In fact, this model had been used as a zero-order approximation in a more general hydrodynamic description of compression-expansion waves propagating in slightly vibrofluidized granular materials [8]. However, when the granular layers are strongly vibrofluidized, the particles' motion is very complicated and differs significantly from the PBM predictions [5,9].

In the majority of works devoted to vibrofluidization, the layer behavior is characterized by kinematic parameters, such as the particle's relative positions and velocities [3–8], the contact time between the layer and the vessel's bottom, and its free-flight duration [3,7,11]. The dynamic layer-vessel interactions, both during the layer motion as a single block and in the vibrofluidized regimes, remain unstudied. The present paper is aimed at bridging this gap. We present experimental data on the forces acting upon the bottom of the vibrating vessel and the work (power) produced on the various layers of inelastically colliding granules.

Measurements of dynamic interactions between the vibrated granules and the vessel are important in design of vibrational machines (e.g., vibromixers), in particular, in calculation of the load exerted by the granules on the vessel, choice of the motor power, calculation of the kinematic parameters of the vibrostand under the load, etc. Knowledge of the forces applied to the vessel together with its displacement allows us to calculate the power supplied to the granular material. Moreover, these measurements are the most effective way to determine several kinematic parameters charac-

*Author to whom correspondence should be addressed. FAX: 972 4 832 45 33. Electronic address: mersm01@tx.technion.ac.il

terizing the layer motion. For example, an efficient way to accurately measure the time of contact between the vessel and the granular material is to measure the duration of the layer's free flight, during which the vessel is unloaded.

Another objective of this investigation is to delineate the applicability of the PBM for characterization of the layer motion, and experimentally identify (by means of the dynamic parameters) those vibrational regimes for which this model is inapplicable. According to the PBM, a granular layer upon touching the vessel instantaneously obtains its velocity. From this moment on and until the detachment, the layer and the vessel have equal velocities without rebound. This time period is called contact time. The layer detachment from the vessel occurs when its acceleration a, is less than the gravitational acceleration, g, i.e., $a<-g$. The time period when the layer freely moves under the action of the gravity force only is called free-flight time. As a model of vibrated layer motion, the PBM does not contain fitting parameters. All vibrational regimes may be characterized by a single dimensionless parameter, namely, dimensionless maximal vibrational acceleration $\Gamma=A(2\pi f)^2/g$, where A and f are the vibrational amplitude and frequency, respectively.

This PBM had been used by mechanical engineers for more than four decades in different modifications [11,12]. It was generalized to a wider class of the so-called single body models which include the layer's viscoelastic impact (viscoelastic model) and air drag force. These modifications require additional coefficients (the drag and damping coefficients, etc.), which cannot be calculated *a priori* but rather found from experiments. Different single body models were tested experimentally wherein the corresponding coefficients served as fitting parameters rather than physical properties [11,12].

In spite of its mathematical simplicity, the PBM sometimes gives the right order of magnitudes of the layer kinematic parameters. Accordingly, it is widely used for practical [12,13] and scientific purposes. In particular, it allows us to describe in terms of parameter Γ several processes, including the transition between different modes of convective flow patterns [6], surface standing waves [3,4], the appearance of transverse waves [7], etc. However, Γ cannot always be used as a sole parameter governing the layer vibroagitation. For example, the intensity of traveling waves [14] or surface waves [15] in vibrated beds strongly depends on *inter alia* vibrational energy of the vessel. In our recent experiments [8,9] we found that for a fixed vessel acceleration, regimes with large A (several centimeters) and small frequencies (less than 20 Hz) are preferable for vibroagitation and mixing of granular materials. This means that for a fixed vessel acceleration, increasing $(Af)^2$ increases vibroagitation and mixing of granular materials.

Several experimental methods were used for study of vibrated beds, including stroboscopic, high speed photography, measurement of the bed electrical conductivity, and the container acceleration [11,3]. The first two methods were used for examination of the layer motion *vis-à-vis* the PBM predictions [11]. Two other methods were used for measurement of the contact time [11,3] and the initial moment of contact [11], respectively. Both methods have clear deficiencies. Measurement of the bed electrical conductivity is efficient for electrically conducting granules only. Measurement of the container acceleration does not enable us to detect the detachment moment.

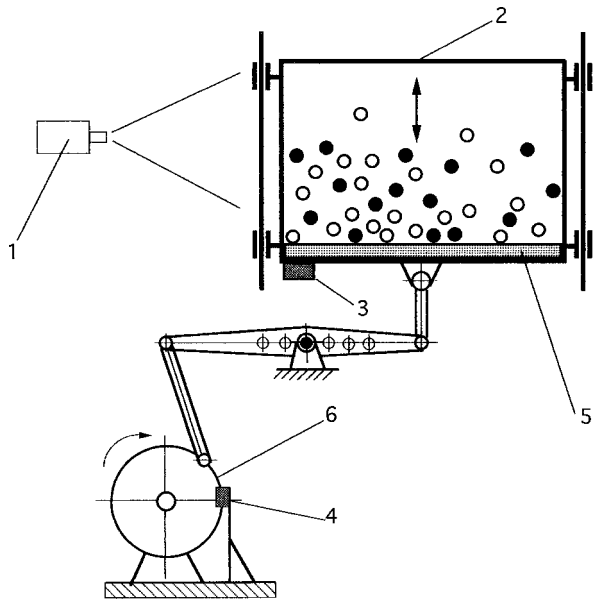

FIG. 1. Schematic of the experimental setup: 1, videocamera; 2, vessel with granular material; 3, accelerometer; 4, pulse transducer; 5, measurement beam; 6, vibrostand drive.

The assumptions underlying PBM may be tested by employing high-speed video photography. This technique had been applied to shallow granular beds [5], where it was found that the bed clears the bottom of the container much later than the PBM predictions. Moreover, significant layer compression and expansion occur during its contact with the vessel and free flight, respectively. This contradicts the PBM assumption that the layer moves as an incompressible single body. As a summary, one can state that no reliable quantitative information on the layer-vessel contact time is known so far.

In the present paper we experimentally investigate the physical mechanisms underlying the vibrofluidization regimes with high amplitudes and low frequencies in a particular case of two-dimensional (2D) granular layers. Since no standard equipment providing controllable vibrations with amplitudes and frequencies in the required ranges is available, a special vibrational stand [16] was designed and constructed, which allows measurements of the kinematic and dynamic parameters of the granular materials.

II. EXPERIMENTAL SETUP

The experimental setup consists of a vibrational stand (see Fig. 1), which provides vertical vibrations of a vessel 2 with a weight of up to 25 kg with controllable frequencies and changeable amplitudes in the respective ranges $0<f<20$ Hz, $0.5<A<5$ cm. The rotational velocity of the electrical motor and the vibrational frequency f are controlled by means of a pulse transducer 4 which consists of a revolving disk with a hole, attached to the flywheel of the drive 6, and a stationary photocell, resting in the vicinity of the disk. This transducer measures the instantaneous rotational velocity with an accuracy of about 0.1%.

According to the kinematic scheme, the vibrostand oscillations were nonsinusoidal. For all results reported below, the vessel maximal acceleration in the downward direction was about 50% larger than the upward maximal acceleration. Further, we will characterize the vessel acceleration with the single parameter $\Gamma = A(2\pi f)^2/g$.

The vessel's time-periodic displacement $x_v(t)$, acceleration $a_v(t)$, and velocity $v_v(t)$ were measured. A system for measurement of the vessel's kinematic parameters was based on a low-frequency accelerometer 3. The accelerometer signal was transferred to a computer and integrated to yield the vessel velocity and displacement. The measured kinematic parameters were used for calculation of displacement, x_p, velocity, v_p, and acceleration, a_p of the layer motion as a single plastic body. Explicitly, the following equations were employed:

$$x_p(t) = x_v(t), \quad v_p(t) = v_v(t),$$

$$a_p(t) = a_v(t) \quad \text{during contact period;}$$

$$x_p(t) = x_v(t_d) + v_v(t_d)(t - t_d) - g(t - t_d)^2/2,$$

$$v_p(t) = v_v(t_d) - g(t - t_d), \quad a_p = -g \quad \text{during free flight,}$$

where the moment of detachment, t_d, is the solution of equation

$$a_v(t) = -g.$$

Vessels (30×45 cm) of several kinds were used, all made of steel frames with transparent glass walls. For the investigation of the disklike particles, the gap between the vertical transparent walls was about 1 mm larger than the disk thickness, to allow their free two-dimensional motion with minimal friction. Here we describe the experiments with one large disk (with diameters 18, 27, and 36 mm) immersed into layers composed of 6–12 ML of small identical disks (with diameter 11 mm) made of the same material, aluminum or brass. The coefficients of restitution of these materials are less than 0.5. This value is typical for the granular materials processed in the majority of vibrational technologies; it differs significantly from almost elastic materials used in the laboratory experiments, for which the wavy phenomena were found [7,8]. The disks' motion within the vessel was recorded by videocamera 1.

The force exerted by the granular material on the vessel bottom was measured by a high-quality steel beam 5 attached to the bottom. The measurements were performed using four strain-gauges attached to the two sides of the beam, which registered with high accuracy the force exerted upon the vessel bottom. The data from the transducers were transmitted to a computer through a data acquisition board, which registered the information with a frequency of 2.5 KHz. A more detailed description on the experimental measurement system can be found in [9].

III. EXPERIMENTAL RESULTS

A. Kinematics of the vibrated layers

The two-dimensional vessels were filled with 6–12 ML of smaller identical disks and one large disk made of the same material. Each series of experiments was performed at constant amplitude with the large disk initially placed on the bottom of the vessel beneath the small disks. It was found that in the majority of regimes the layers oscillate periodically, however sometimes aperiodic motion occurs (see below).

Figures 2(a)–2(e) present photographs of the characteristic vibrational regimes observed in the study. At low frequencies the layers remain attached to the bottom [nondetaching regime, Fig. 2(a)]. At higher frequencies they detach from the bottom and prevail in a free flight during some parts of the vibrational period [detaching regime, Fig. 2(b)]. Further increase of the vibrational acceleration leads to diminution of the time of contact with the vessel to the extent which allowed viewing the layer-vessel interaction as bouncing [bouncing regimes, Figs. 2(c)–2(e)]. Such bouncing is accompanied by the layers' periodic expansion and contraction, and also distortion of their free surfaces as a result of the transverse gravitational waves [7,8].

One interesting peculiarity of the layer motion in the detaching regimes is the so-called repacking phenomenon, observed in this study. Namely, for each amplitude there exists a certain narrow acceleration range, lying within the bouncing domain, where the particles' intensive relative motion terminates and they collapse into a solid block [see Fig. 3(a)], which periodically jumps off the vessel bottom. With increasing acceleration this repacking disappears, although this phenomenon is also observed at a higher acceleration, albeit in a less pronounced manner, since the layer motion in this regime is significantly affected by the transverse waves [see Fig. 3(b)]. The frequencies at which the particles' repacking had been registered are further related to the PBM predictions (see below).

The above regimes were also characterized by the motion of the large disk immersed in the layer. In the nondetaching and detaching regimes (*A* and *B*, see Fig. 4 below) this disk remains essentially at the vessel's bottom, where it was initially placed. Beginning from a certain acceleration, an intensive relative particle motion begins, which brings the large disk to the layer upper surface, where it continues to move without penetrating back into the layer. This is a manifestation of the well-known ''Brazil nuts'' effect, which is segregation of larger particles on top of vibrated layers composed of smaller ones. This segregation regime *C* prevails with increasing acceleration until the repacking regime is reached.

When the vibrational acceleration is further increased, the layer expands again and the transverse waves affect dramatically the large particle's motion. These waves make it dive deeply into the layer and move in a chaotic manner, sampling all possible positions within the layer with about equal probability. That is, the effect of these waves is to eliminate the segregation, thereby providing conditions potentially beneficial for particle mixing. This mixing regime *D* prevails in the acceleration range until the second repacking is reached.

Figure 4 depicts the layer kinematic map plotted in terms of the vibrational amplitude *A* and the dimensionless acceleration Γ. One can see that the boundaries of the regimes are almost independent of the amplitude. One can thus characterize the basic layer regimes with respect to the large par-

FIG. 2. Photographs of vibrational regimes (amplitude $A=25$ mm) observed in the study: (a) $f=1$ Hz, nondetaching motion; (b) $f=3.8$ Hz, detaching regime; (c) $f=5.2$ Hz, segregation regime; (d) $f=8.5$ Hz, mixing regime; (e) $f=9.3$ Hz, mixing regime. (c)–(e) Bouncing layer motion.

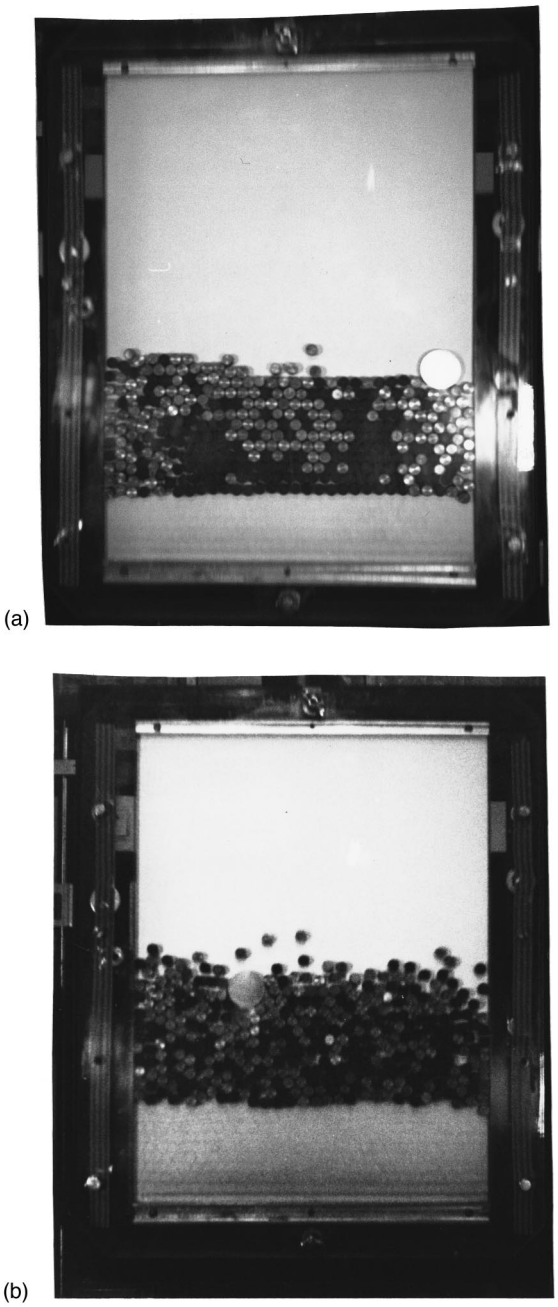

FIG. 3. Photographs of repacking phenomenon (amplitude $A=25$ mm): (a) $f=7.1$ Hz, first repacking; (b) $f=9.1$ Hz, second repacking.

ticle motion in the following universal way:

A: $0<\Gamma<1.2$, nondetaching regime,

B: $1.2<\Gamma<2.4$, detaching regime without relative motion between the large disk and the layer,

C: $2.4<\Gamma<5$, segregation regime (upward motion of the large disk),

D: $5<\Gamma<8.5$, vibromixing regime (chaotic motion of the large disk),

E: $\Gamma>8.5$.

The first and the second repacking regimes prevail in narrow ranges around the respective dimensionless accelerations $\Gamma=5$ and 8.5. We found that both characteristic ''repacking'' accelerations are predictable by the plastic body model. Namely, at these accelerations the relative velocity between the body and the vessel at the moments of their contacts is minimal (see below, Fig. 6). More recently, we have revealed that in a close vicinity of the first repacking, motion of the large disk significantly differs from that prevailing in regimes *C* and *D*. These results together with the experimental investigation of vibromixing are to be reported elsewhere [17].

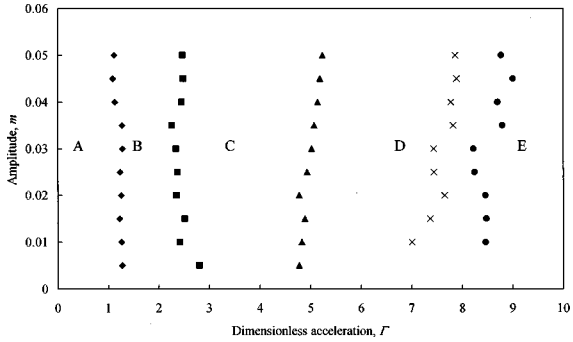

FIG. 4. Kinematic map of vibrofluidization regimes for vibrated 2D layers composed of 6–12 ML. *A*, nondetaching regime; *B*, detaching regime (no relative motion); *C*, segregation regime; *D*,*E*, mixing regimes. Triangles, circles, and crosses correspond to first and second repacking regimes and the regime of most vigorous vibromixing, respectively.

In a recent study [3] the authors describe surface waves' patterns of 3D vibrated layers observed from above. We compared the acceleration ranges of the regimes that we observed on our 2D layers with the ranges of Γ where different patterns of 3D layers prevailed, as reported in [3]. Analysis of these patterns shows that the regime yielding a pattern where the upper surface of a 3D layer consists of flat domains separated by a discontinuity line (kink) is close the acceleration range where the repacking regime in our 2D layers prevails. Furthermore, speaking in terms of acceleration range, our 2D segregation regime corresponds to 3D ''$f/2$ waves and hexagons''; our mixing regime corresponds to ''$f/4$ waves and hexagons'' observed in [3]. Our detaching regime *B* corresponds to the ''flat layer'' regime reported in [3]. The small differences in boundary values of the dimensionless acceleration between the concomitant regimes may be attributed to the difference in the forms of the vibrational excitations. The surface wave patterns were investigated in [3] for the sinusoidal (harmonic) oscillations, while the experimental results reported here were collected for nonsymmetric vibrational excitations (see the preceding section).

The surface waves occurring on top of the vertical granular layers constitute the motion of two or three upper monolayers of a whole vibrated layer and are rather independent of the layer depth and insensitive to the particle properties [3]. The surface waves' regime as expressed by the vibrational acceleration range is insufficient for the full characterization of the layer vibrofluidization, since the latter includes both the layer expansion and intensive relative motion of granules. Vibrofluidization is a result of the balance between the energy input from the vibrating vessel and the energy losses due to inelastic collisions. These losses, generally speaking, increase with increasing particle number and inelasticity of their collisions [8]. Since the surface waves are insensitive to the energy losses, they at most serve as an indication of

fluidization of a thin surface part of the vibrated layer but not the whole layer.

Fluidization of a thin surface part of the vibrated layer can be visualized from above with a video camera. Such observations do not allow visualization particles' relative motion in the remaining part of the layer and, in particular, the motion of a large particle when it ''dives'' into the layer. In order to get such information, we observed and videorecorded 2D layers from the side which enables us to track the motion of any particle within the layer. The two methods of visualization, namely from the side and from the top, are complimentary in nature; their combination gives insight about the overall behavior of the vibrated layer from the bottom to the top. For example, the kink phenomenon, which had been registered by videorecording the upper surface of 3D layers [3], shows that no relative particle motion occurs on the top for $\Gamma=5.8$ (flat domains connected by a kink). For the same vibrational regime, we registered by means of side videorecording no relative motion in the whole granular layer [see Fig. 2(d)].

Another advantage of side videorecording with respect to top videorecording is in the observation of transverse waves [7,8]. These waves manifest themselves through bending of the *whole* layer and can hardly be registered by any observations from above. Our experiments revealed that there exists a correlation between the layer bending and the intensity of the motion of the large disk within the bed, characteristic of the mixing process. In particular, the most vigorous ''vibromixing'' has been registered in the vibrational regimes where the amplitude of the transverse wave is maximal. These regimes are marked in the map shown in Fig. 4 by cross symbols. In passing, we will note that our measurement of contact time (see below) showed that for the intensive vibromixing regimes the vibrated layer contacts the vessel *once* per vibrational period. This contradicts the PBM predictions yielding one layer contact per *two* vibrational periods.

The representation of the vibrational regimes given in Fig. 4 is valid for sufficiently large amplitudes, as predicted by the condition that the parameter $V=A\omega/(gh)^{1/2}$ is of order one [8]. In the present case this condition is already fulfilled for $A\geqslant 5$ mm for all layer heights h tested. However, these regimes are to be tested for wider ranges of the layer heights and granular properties. For small amplitudes the second repacking is very difficult to achieve, since it occurs for very large frequencies. According to the PBM predictions, for 1 mm amplitude the second repacking occurs at about $f\sim 46$ Hz, which is beyond the capability of our vibrational stand.

B. Force measurements

The plastic body model does not enable us to distinguish between regimes *B* and *C*. This may be done, however, on the basis of the force measurements. Figure 5 shows the time evolution of the force exerted on the vessel bottom by the granular material. One can see that for the frequency 3.89 Hz, corresponding to the detaching regime *B*, the vessel is loaded during about 40% of the vibrational period in two portions: one is a short blow in the vicinity of the dimensionless time moment $tf\sim 0.4$ lasting about 3.5% of the period,

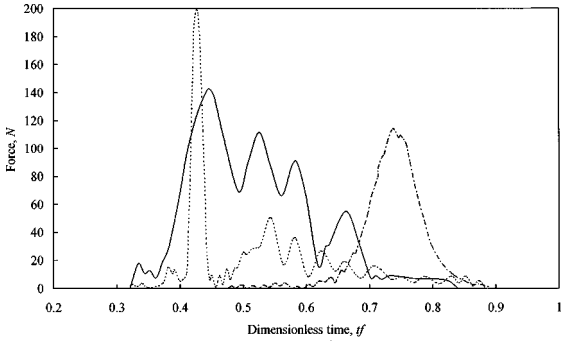

FIG. 5. Time evolution of the force exerted on the vessel bottom by the granular material for several frequencies: $A=25$ mm, 6 ML of brass disks of diameter 11 mm. Dotted, dashed-dotted, and solid curves correspond to the following frequencies: $f=3.89$ Hz (regime *B*), $f=6.01$ Hz (regime *C*), and $f=6.95$ Hz (the first repacking regime), respectively.

and another is a continuous load for $0.45<tf<0.85$, where the layer is attached to the bottom. For the frequency $f=6.01$ Hz, corresponding to the *C* regime, the load is applied as a single blow lasting about 20% of the period. A similar behavior of the force was registered also in close vicinity to the frequencies corresponding to the first repacking. The bouncing regimes *C,D,E* are characterized by a single blow during each layer-bottom interaction, which justifies this terminology.

The transition from the detaching to the bouncing regime may also be characterized by means of the force measurements. Figure 6(a) shows the maximal force acting during one vibrational period on the vessel plotted versus the vibration acceleration for the amplitude $A=25$ mm. One can see that this force reaches its maximal value within region *B*. This value exceeds the layer weight by more that 30 times for $\Gamma=2$. This acceleration characterizes the transition from the detaching to the bouncing regime (see the discussion below). This transition occurs at Γ smaller than the acceleration of the transition to the segregation regime *C* for all our measurements (see Fig. 6).

It is noteworthy that in the vicinity of the boundary acceleration $\Gamma=2$, the layer behavior repeats itself every second period. That is, the layer dynamics is different during even and odd periods. We call this phenomenon ''dynamic bifurcation.'' This bifurcation prevails for $1.7<\Gamma<2.2$. The second dynamic bifurcation appears for higher accelerations between the first and second repackings. This bifurcation phenomenon was rationalized by the kinematic PBM.

The layer motion as prescribed by the PBM (see Sec. II) was calculated numerically for the vessel displacement $x_v(t)$, acceleration $a_v(t)$, and velocity $v_v(t)$ obtained from the measurements of 50 consequent periods of the vessel oscillations. For each of them the period of contact $t_c^{(i)}$ and the period of free flight $t_f^{(i)}$ $(i=1,2,...,50)$ were calculated $(t_c^{(i)}+t_f^{(i)}=T)$. It was found that in the majority of the regimes the layer oscillates periodically. Unlike the case of the sinusoidal law of the vessel motion [12], we observed regimes with one contact of the body per one period: $t_c^{(i)}=t_c^{(i+1)}$, per two periods: $t_c^{(i)}=t_c^{(i+2)}$, $t_c^{(i+1)}=0$, and per three periods: $t_c^{(i)}=t_c^{(i+3)}$, $t_c^{(i+1)}=t_c^{(i+2)}=0$, of the vessel oscillations. We also found nonperiodic regimes with con-

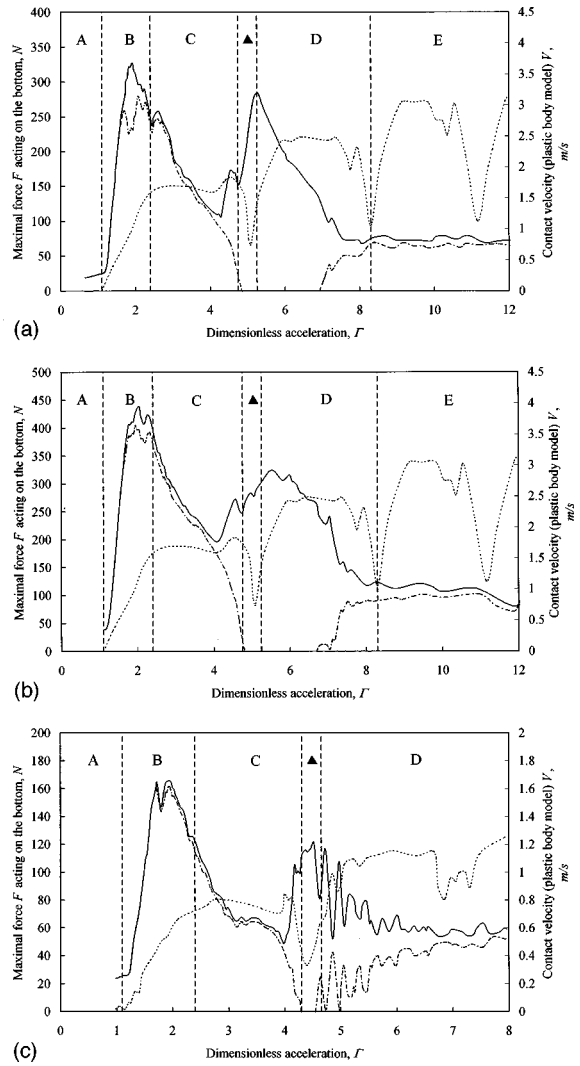

FIG. 6. Maximal force acting on the vessel's bottom versus the vibrational dimensionless acceleration. The bed is composed of brass disks with an 11-mm diameter. Solid and dashed-dotted lines correspond to measurements of odd and even periods, respectively; dotted lines correspond to layer-vessel relative velocity prior to the contact (calculations using PBM). (a) 6 ML, vibrational amplitude $A=25$ mm; (b) 10 ML, vibrational amplitude $A=25$ mm; (c) 6 ML, vibrational amplitude $A=5$ mm. Acceleration regions *A,B,C,D,E* correspond to the regimes marked in Fig. 4; triangles (between the regimes *C* and *D*) correspond to the first repacking regime.

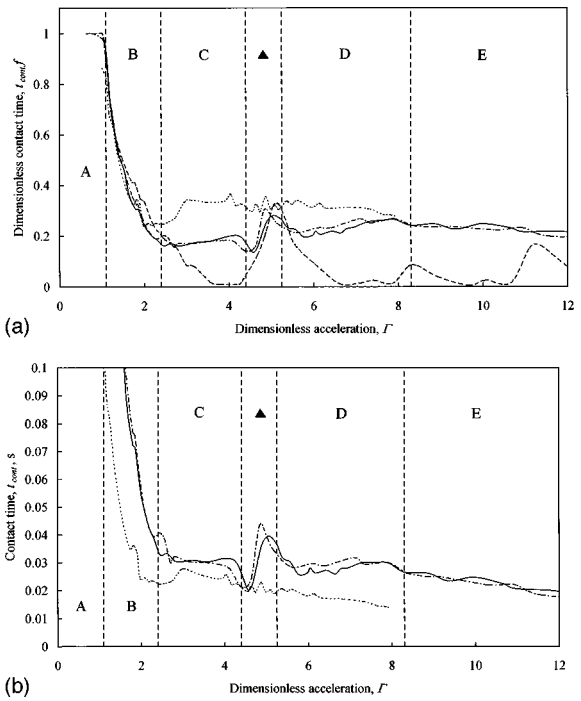

FIG. 7. Contact time between the layer (brass disks with a diameter of 11 mm) and the vessel's bottom versus the vibrational dimensionless acceleration. Dashed-dotted lines, 6 ML, vibrational amplitude $A=25$ mm; solid lines, 10 ML, vibrational amplitude $A=25$ mm; dotted lines, 6 ML, vibrational amplitude $A=5$ mm; dashed line, predictions of PBM: (a) dimensionless, (b) dimensional. Acceleration regions *A,B,C,D,E* correspond to the regimes marked in Fig. 4; triangles (between the regimes *C* and *D*) correspond to the first repacking regime.

stantly varying layer-vessel periods of contact.

Figure 6(a) shows the plot of the layer-vessel relative velocity V, calculated on the basis of the PBM. One can see two minima of V for $\Gamma=5.08$ and 8.3 corresponding to the first and second repackings, respectively. The second repacking is very unstable because of the transverse waves, and can hardly be registered by the force measurement. For large accelerations, the maximal forces as measured during all (odd and even) periods are both close to the average force value over one period. In this range the layer behavior is characterized by intensive transverse waves.

The force measurements presented in Figs. 6(a)–6(c) are the result of time averaging over the period of 15 s, which includes many vibrational periods. The maximal scatter of the measured force was registered for the regimes of the dynamic bifurcation and transverse waves. This large scatter allows us to explain why the force measurements fail to register the second repacking regime, observable and predictable by the PBM. The lifetime of the second repacking regime is of the order of several vessel oscillations. This time period is long enough to allow observation of repacking, but much smaller than the averaging period. Hence, the repacking produces no effect on the average force values.

One can see in Fig. 6 that the first repacking regime takes place in a relatively narrow acceleration range from $\Gamma=4.75$ to 5.25. The beginning of this range may be estimated by a local minimum, and its end by a local maximum of the force F. This range contains the acceleration $\Gamma=5.08$, at which, according to the PBM predictions, the layer-vessel relative velocity is minimal. Below (see Fig. 7) we estimate the acceleration range of the first repacking regime on the basis of measurements of the contact time and show that it is close to the comparable range observed in Fig. 6.

The effects of the vibrational amplitude and the layer depth on the maximal force are depicted in Figs. 6(b) and 6(c). Many of the conclusions which have been drawn from Fig. 6(a) equally apply also for the deeper layers [Fig. 6(b)] and smaller vibrational amplitudes [Fig. 6(c)].

We used the data measured on the forces to verify the contact time predictions made on the basis of the PBM. Figures 7(a) and 7(b) show the dimensionless [Fig. 7(a)] and dimensional [Fig. 7(b)] contact time between the layer and the vessel, plotted against the vibration acceleration for two

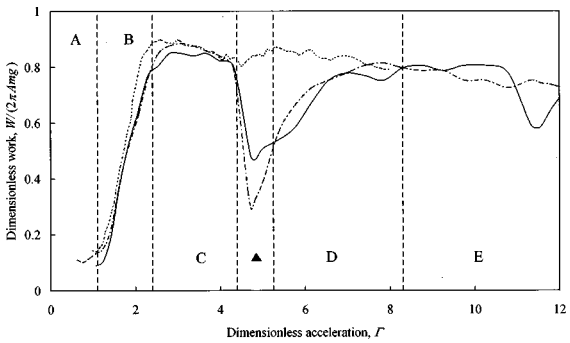

FIG. 8. Work performed on the granular layer during one period vs vibrational acceleration (brass disks of diameter 11 mm). For the lines' descriptions, see the caption for Fig. 7.

amplitudes and two layer heights. The characteristic vibrational regimes are also clearly distinguished in this figure, which, in addition, shows the contact time predicted by the PBM [Fig. 7(a)]. One can see that the PBM predictions are close to the experimental data in the detaching regime *B* and significantly differ in the bouncing regime. The difference is most remarkable for those regimes where the model predicts one contact per two periods. In contrast to this prediction, we registered one contact per period. Moreover, for each period the contact time is almost the same. Such disagreement between theory and experimental data is explained by the layer bending and appearance of the transverse waves [7]. For such regimes the PBM is, apparently, inapplicable.

In the vicinity of Γ corresponding to the first repacking, the layers again behave in accordance with the PBM predictions. Beyond the repacking regime the dimensionless contact time of the granular layers is larger than the calculated values. The dimensionless contact time is almost independent of the layer height, but depends on the vibrational amplitude.

For 5 mm amplitude, the transverse waves appear in the bouncing regime for lower accelerations than those registered for $A=25\,\mathrm{mm}$. As a result, the contact time t_c for the 5 mm amplitude regime is significantly larger than for the 25 mm regime. In the acceleration range above $\Gamma=7.8$, where the motion of all layers is affected by the transverse waves, the dimensionless contact times for both amplitudes are close to each other, albeit both exceed significantly the PBM prediction, which clearly does not account for these waves. For the transverse waves appearing in regimes *D* and *E*, the product $t_c f$ is almost independent of the layer height and the vibrational amplitude, but grows linearly with Γ in the range $7.8<\Gamma<18$, where it takes the values $0.2<t_c<0.3$ (in Fig. 7 we present only a part of our measurements).

Figure 7(b) shows the contact time between the layer and the vessel, plotted against the vibration acceleration for two amplitudes and two layer heights. One can see that after the first repacking regime the contact time again varies linearly with Γ with the linearity coefficient being practically independent of the vibrational amplitude. In regime *C*, the contact times for both amplitudes are close to 0.03 s, which exceeds significantly the PBM prediction.

C. Work performed on vibrated granular layers

Figure 8 shows the dimensionless work $w=W/2\pi Amg$ performed on the granular layers during one period. Many of the conclusions which have already been drawn from Figs. 6 and 7 equally apply also to this plot. In particular, the work seems to be independent of the vibration amplitude and the layer height in the acceleration range prior to the beginning of the first repacking. This work is larger for the bouncing regimes than for the detaching or repacking regimes. In the bouncing regimes the dimensionless work slightly decreases with Γ, and it is almost independent of the layer height, at least in the range of heights investigated (see the two curves in Fig. 8 obtained for 25 mm amplitude and heights of 6 and 10 ML). In the vicinity of the repacking regime with 25 mm amplitude, a lower work is measured than that registered for 5 mm amplitude. This may be rationalized by noting that for the latter amplitude the repacking regime is difficult to achieve, since it is easily broken by the transverse waves. Accordingly, the work performed to sustain the layer in the fluidized state is larger for the 5 mm regime than for the 25 mm regime (see Fig. 8), where the repacking is stable.

The maximal work performed during one period may be approximated by a constant value of about $5.5Amg$. So, the larger the vessels' vibration amplitude, the larger work on the granular layer it performs during one period.

IV. DISCUSSION

The results presented in Figs. 7(a) and 7(b) demonstrate that the PBM gives a satisfactory description of the kinematic layer motion for nondetaching, detaching, and repacking regimes. This may be explained on the basis of our theory of vibrofluidization of granular materials by vertical vibrations [8]. It was shown that for efficient fluidization it is necessary to *increase* the relative layer-vessel velocity and, hence, the maximal vibrational velocity $A\omega$. On the other hand, the inverse statement is also valid: smaller relative velocity corresponds to lower layer porosity (solid body behavior).

According to the PBM, the layer's (solid body) motion is characterized by instantaneous changes of the layer velocity at the moments of contact with the vessel bottom. In addition, the model assumes no bouncing after impacts. In fact, we registered *several* fast impacts of granular layers with the vessel during one period, which are manifested as peaks of the force for detaching and repacking regimes (see Fig. 5). These multiple impacts may be explained on the basis of a more general model of the motion of a solid body with a nonzero coefficient of restitution *e* [12]. In reality, the effective value of *e* of the whole granular layers depends on the vibrational regime, layer height, collisional particle properties, etc. These dependencies are usually determined form the experimental data [12]. However, the contact period, which in the case of several impacts is the sum of all impact times, usually depends only slightly on these data. This justifies the use of the PBM for the modeling of kinematic parameters of the vibrated layers.

More elaborate models of the layer-vessel interactions take into account the time of propagation of disturbances across the layers. It is commonly believed that the speed of sound propagation in granular systems depends on the layer depth [18]. Since the most significant spatial variations of the layer density and granular temperature are mainly in the ver-

tical direction, measurement of the speed of sound in this direction yields only averaged values. On the other hand, disturbances propagating in the horizontal planes pass through more homogeneous particle arrangements. Hence, measurements of the speed of sound in the horizontal direction may be better characterized. In particular, for a granular material consisting of 5 mm glass beads, such measurements yield the speed of a single pulse propagation, about 280 m/s [18]; and the group velocity, about 57 m/s [19]. This speed was also measured for small disturbances [19], where it was found to be very sensitive to the layer structural changes. Below we compare this group velocity with the propagation speed of the compression waves [11] in vibrated granular beds.

Estimations of the average value of this velocity may be done on the basis of our experimental data of the force evolution (see Fig. 5). The first peak in the curve occurring at $f=3.89$ Hz may be attributed to propagation of compression/expansion waves in the granular system. Hence, these waves propagate to a distance of the order of two layer heights (up and down), i.e., about 0.13 m over about 0.009 s. The ratio of these values, i.e., 15 m/s, gives a rough estimation of the average speed of the wave propagation, v_{av}. Similar calculations for other experimental data (not presented here) show that v_{av} varies within the range of 12–20 m/s depending on the layer height and vibrational parameters. Consequently, v_{av} is several times slower than the group velocity in granular materials obtained in [19].

The reason for the above discrepancy is that in our systems the layer density is lower due to vibrofluidization. This may be illustrated by the following formula [20]:

$$V_s=\frac{U}{1-\rho_0/\rho_m}, \tag{1}$$

which allows calculation of the speed V_s of the shock wave caused by a piston moving with velocity U into a granular gas of initial (undisturbed) density ρ_0, and ρ_m is the maximum density. Use of this formula in the circumstances of vibrated granular layers is difficult since the ''initial'' density ρ_0 (i.e., the one prevailing prior to the layer contact with the vessel) depends on the vibrational regime. In the present experiments the difference $\Delta=1-\rho_0/\rho_m$ was of order 0.1. Taking this value as a fair estimate of the layer density and identifying U in Eq. (1) as the piston's maximal velocity, one obtains that $V_s\sim 10A\omega$. Noting that in the wave propagating regime $A\omega$ is of order 1–2 m/s, one can see that the above expression gives $V_s\sim 10-20$ m/s, which is of the same order of magnitude as the estimates made on the basis of Fig. 5.

On the other hand, one can use the expression for the *average* shock wave speed predicted by the semiempirical theory of vibrofluidization of a granular layer of height h [8]:

$$V_s=\frac{2}{\kappa(H)}\frac{gh}{A\omega}, \tag{2}$$

wherein κ is a coefficient calculated in [8] and dependent on the parameter

$$H=1.02(1-e^2)h/\sigma.$$

This expression is free of the ambiguity characteristic of formula (1), since it does not contain unknown parameters. Indeed using $e\sim 0.3$ as for brass particles and $h/\sigma=6-10$ ML, one obtains $H\sim 5.5-10$. Using this value and calculations performed in [8], one obtains that $\kappa\sim 0.1$, which yields the shock wave velocity $V_s\sim 6-20$ m/s. This is consistent with both of the above estimates, i.e., those based on formula (1) and on the experimental data in Fig. 5.

The time of vessel-layer interaction t_{cont} depends in a complicated manner on several parameters, in particular on the relative layer-vessel velocity prior to the contact. The average speed of the wave propagation v_{av} may be used to estimate t_{cont}, as the time during which the compression-expansion waves travel, respectively, up and down the layer height: $t_{\mathrm{av}}\sim 2h/v_{\mathrm{av}}$. The PBM predicts the dimensionless time of contact t_{PBM} varying from 0 to 1 [see Fig. 7(a)]. It might be expected that this model is valid as long as t_{PBM} is larger that t_{av}. One can see in Fig. 7(a) that t_{PBM} significantly underestimates the measured contact time t_{cont} beginning from about $\Gamma=2.5$, where they both close to 0.03 s. This may be compared with the estimations made on the basis of the shock wave speed, which yield $t_{\mathrm{av}}\sim 0.01$ s. This points out that the wave propagation model gives the right order of magnitude of t_{cont} in the bouncing vibrofluidized regimes.

The breakdown of the PBM is due to the layer fluidization, i.e., increasing layer porosity. Our videorecordings show that in the bouncing regime the granules separate from each other during the free-flight period. They do not fully collapse onto the vessel bottom during the contact period. The layer bouncing occurs over a relatively long period, which depends on the layer density prior to meeting with the vessel. The layer density ρ in the bouncing regime differs insignificantly from the maximal repacking density ρ_m and such deviations can hardly be measured with sufficient accuracy. However, it is well known from the simple dense fluids theory [21] that small changes of ρ lead to significant changes of the pressure, since the latter is inversely proportional to $\Delta=1-\rho/\rho_m$. For a dense system of rigid particles it is easier to measure forces than densities. That is why here we use force measurements rather than density measurements in order to characterize the vibrational regimes.

In the bouncing regime, the maximal force F_{max} and the contact period t_{cont} are correlated. Indeed, for a layer which periodically experiences a vertical force $F(t)$ applied by the vibrating vessel, one obtains

$$\int_0^T F(t)dt=mgT, \tag{3}$$

where m is the layer mass, T is the oscillation period, and g is the gravitational acceleration. The integral on the left-hand side of Eq. (3) may be evaluated in the following form:

$$\int_0^T F(t)dt=kF_{\mathrm{max}}t_{\mathrm{cont}}, \tag{4}$$

where the coefficient k depends on the specific form of the function $F(t)$. For example, for the rectangular force distribution form one has $k=1$; for the parabolic distribution form, $k=\frac{2}{3}$; for the triangular distribution form, $k=\frac{1}{2}$; and

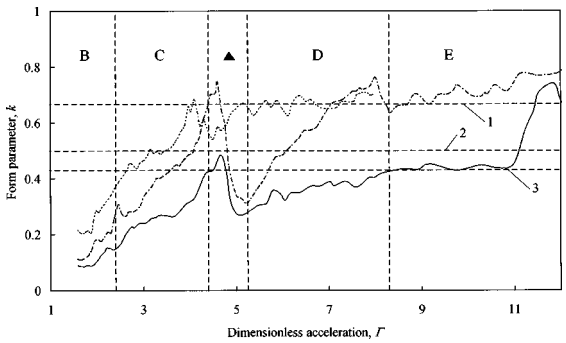

FIG. 9. Form parameter k characterizing the force evolution versus the acceleration (brass disks with diameter of 11 mm). Horizontal dashed lines: 1, parabolic form distribution; 2, triangular form distribution; 3, normal form distribution. For the lines' descriptions, see the caption for Fig. 7.

for the normal distribution form, $k=0.414$. The latter value is obtained under the constraint that 99% of the value of this integral is provided by the force integration over t_{cont}. Coefficient k may be calculated on the basis of our experimental data. Towards this goal Eqs. (3) and (4) combine to give

$$k=\left(\frac{F_{\max}}{mg}\frac{t_{\mathrm{cont}}}{T}\right)^{-1}, \tag{5}$$

which implies that k is inversely proportional to the normalized maximal force and time of contact. Using the data for the maximal force from Fig. 6 and for the dimensionless contact time from Fig. 7(a), one can calculate k from relation (5). The results of such calculations together with the analytical solutions for the model force distributions are presented in Fig. 9. One can see that for small vibrational amplitude $A=5$ mm, k increases monotonically with increasing vibrational acceleration. For large amplitude $A=25$ mm, k depends on Γ in a similar manner, except for a small acceleration region within the first repacking regime, where k rapidly decreases with Γ. Coefficient k decreases with increasing layer height and/or vibrational amplitude (for a fixed vibrational acceleration).

Now we discuss the energy aspects of the vibrofluidized granular beds. Using integral estimations, one can express the work W performed by the vessel on the granular layers during one period in the form

$$W=\int_0^T v(t)F(t)dt=\tilde{v}\int_0^T F(t)dt=\tilde{v}mgT, \tag{6a}$$

where $v(t)$ is the vessel velocity and $\tilde{v}$ is the vessel velocity at a certain moment during the contact period. One can write $\tilde{v}$ in the following form:

$$\tilde{v}=k_w A 2\pi/T, \tag{6b}$$

where the coefficient $k_w \leqslant 1$. Relations (6) allow us to express the dimensionless work in the form

$$w=\frac{W}{2\pi Amg}=k_w, \tag{7a}$$

According to Eq. (7a), the dimensionless work is smaller than 1. Since we consider periodic motion of the granules, all this work is lost (converted to heat) during one period. Coefficient k_w characterizes the energy losses within the granular layers during one period. When such losses are absent, k_w is equal to zero. The larger this coefficient, the larger the energy losses.

On the other hand, the layer cannot lose more energy that it gets from the vibrating vessel. For the sake of comparison between different vibrational regimes we introduce the effective power of the vibrated vessel, $N=W/T$. Formula (7a) may be rewritten in terms of N as

$$\frac{N}{mgV_{\max}}=k_w, \tag{7b}$$

where $V_{\max}=2\pi A/T$ is the maximal vibrational velocity. According to Eq. (7b) the power is proportional to the maximal vibrational velocity. The larger this velocity, the larger the power transferred to the granular layer and, hence, the better vibrofluidization may be achieved. This conclusion agrees with our earlier results [8] and the experimental finding of [14,15].

McNamara and Luding [22] studied equilibrium states of the vibrated granular layers. In particular, they used scaling (7b) for the energy input by a vibrating floor. They suggested that the coefficient k_w depends only on the ratio $U/V_{\max}$, where U is proportional to the square of the average energy of chaotic granular motion. We did not measure this energy, but our observations show that it is smaller for the repacking regime than that for the vibromixing regime. On the other hand, our measurements of k_w imply that k_w is smaller for the repacking regime than that for the vibromixing regime. These observations and measurements give support to the scaling suggested in [22]. One should note, however, that this scaling is not universal, since it ignores the effect of parameter Γ, governing the transition between the vibrational regimes.

V. CONCLUSIONS

We found new and interesting phenomena in the behavior of vibrated 2D layers of granular materials. These are repacking regimes (no relative motion of granules under action of intensive vibration) and ''vibromixing'' regimes (chaotic motion of a single large particle). These and other vibrational regimes, namely the nondetaching regime and the segregation regime (upward motion of the large disk), are indicated in the map plotted in terms of vibrational amplitude and acceleration. These regimes, expressed in terms of the dimensionless acceleration, may also be characterized by the wave patterns which were observed on the upper surfaces of 3D layers [3].

We found that repacking and detaching regimes are predictable by the plastic body model. These regimes were shown to correlate with the minima of the work produced by the vibrated vessel. On the other hand, regimes of intensive vibrofluidization (segregation and ''vibromixing'' regimes) were found to correlate with the minimum of the load exerted upon the vessel by the granular material and a maximal value of the work per unit of time (power). The latter value is

found to be proportional to the maximal vibrational velocity with a coefficient only slightly dependent on the layer height, vibrational amplitude, and acceleration.

Time of contact t_{cont} between the layer and vessel was measured for all investigated regimes. This time was found to be underestimated by the analysis for the bouncing regimes performed using the plastic body model. This discrepancy between the experimental data and PBM predictions is due to compression-expansion wave propagation within vibrated granular layers. The speed propagation of these waves was estimated and shown to be several times smaller than the speed of sound waves in sand, reported in the literature.

The vibromixing regimes were observed for materials with collisional properties close to those of real granular materials. These regimes are beneficial for the design of technological equipment for vibromixing, characterized by the minimum load and, hence, lower capital costs, operating expenses, and a longer lifetime. These regimes need further experimental and theoretical investigations.

ACKNOWLEDGMENTS

This research was supported by the Israel Science Foundation administered by the Israel Academy of Sciences and Arts, by the Center of Absorption in Science and the Gilliady Program for Immigrant Scientists Absorption, by the Fund for the Promotion of Research at the Technion, and by the Technion V.P.R. Fund–Smoler Research Fund. The authors are thankful to Galina Shapiro for providing her home videocamera for videorecordings of granular regimes. A.G. is grateful to S. R. Nagel for his hospitality and for providing his stimulating paper on sound propagation in sand, and L. Kadanoff, H. M. Jaeger, and other members of the University of Chicago, MRSEC for stimulating discussions.

[1] B. J. Ennis, in *Powders & Grains 97*, Proceedings of the Third International Conference on Powders and Grains, edited by R. P. Behringer and J. T. Jenkins (A. A. Balkema Publishers, Rotterdam, 1997), pp. 13–23.

[2] H. M. Jaeger, S. R. Nagel, and R. P. Behringer, Rev. Mod. Phys. **68**, 1259 (1996).

[3] H. L. Swinney, P. B. Umbanhowar, and F. Melo, in *Powders & Grains 97* (Ref. [1]), pp. 369–372; B. Umbanhowar, F. Melo, and H. L. Swinney, Nature (London) **382**, 793 (1996); F. Melo, B. Umbanhowar, and H. L. Swinney, Phys. Rev. Lett. **75**, 3838 (1995); C. Bison, M. D. Shattuck, J. B. Swift, W. D. McCormic, and H. L. Swinney, *ibid.* **80**, 57 (1998).

[4] S. Luding, E. Clement, J. Rajchenbach, and J. Duran, Europhys. Lett. **36**, 247 (1996).

[5] T. Metcalf, J. B. Knight, and H. M. Jaeger, Physica A **236**, 202 (1997).

[6] Y-h. Taguchi, Phys. Rev. Lett. **69**, 1367 (1992); K. M. Aoki, T. Akiyama, Y. Maki, and T. Watanabe, Phys. Rev. E **54**, 874 (1996).

[7] S. Doudy, S. Fauve, and C. Laroshe, Europhys. Lett. **8**, 621 (1989).

[8] A. Goldshtein, M. Shapiro, L. Moldavsky, and M. Fichman, J. Fluid Mech. **287**, 349 (1995).

[9] V. Royzen, V. Dudko, A. Alexeev, A. Goldshtein, and M. Shapiro, in *Proceedings of the Second Israel Conference for Conveying and Handling of Particulate Solids*, edited by H. Kalman (International Convention Center, Jerusalem, 1997), p. 11.23.

[10] B. Thomas, M. O. Mason, Y. A. Liu, and A. M. Squires, Powder Technol. **57**, 267 (1989); B. Thomas and A. M. Squires, in *Fluidization IV*, edited by J. R. Grace, L. W. Shemilt, and M. A. Bergoughou (Benif, Alberta, Canada, 1989).

[11] W. A. Gray and G. T. Rhodes, Powder Technol. **6**, 271 (1972).

[12] I. I. Blekhman and D. G. Dzhanelidze, *Vibrational Transport* (Nauka, Moscow, 1964); K. Erdesz and J. Nemeth, Powder Technol. **55**, 161 (1988).

[13] I. Gutman, *Industrial Uses of Mechanical Vibrations* (Business Books, London, 1968); V. A. Chlenov and N. D. Mikhailov, *Vibrofluidized Beds* (Nauka, Moscow, 1972).

[14] H. K. Pak and R. G. Behringer, Phys. Rev. Lett. **71**, 1832 (1993).

[15] C. R. Wassgren, M. L. Hunt, and C. E. Brennen, in Ref. [1], pp. 13–23 and 433–436.

[16] V. Royzen, V. Dudko, A. Goldshtein, and M. Shapiro, in *Proceedings of the 26th Israel Conference on Mechanical Engineering, Haifa*, edited by A. L. Yarin (Technion City, Haifa, 1996), p. 225.

[17] V. Royzen, A. Goldshtein, and M. Shapiro (unpublished).

[18] C-h. Liu and S. R. Nagel, Phys. Rev. Lett. **68**, 2301 (1992).

[19] C-h. Liu and S. R. Nagel, J. Phys.: Condens. Matter **6**, A433 (1994).

[20] A. Goldshtein, M. Shapiro, and C. Gutfinger, J. Fluid Mech. **316**, 29 (1996).

[21] B. J. Alder and W. G. Hoover, in *Physics of Simple Liquids* (North-Holland, Amsterdam, 1968), pp. 79–114.

[22] S. McNamara and S. Luding, Phys. Rev. E **58**, 813 (1998).